EFFECTS OF THE EQUATORIAL IONOSPHERE ON L-BAND EARTH-SPACE TRANSMISSIONS

by
Ernest K. Smith and Warren L. Flock
NASA Propagation Information Center
ECE Department, University of Colorado
Boulder, Colorado, 80309

Abstract
Ionosphere scintillation can effect satellite telecommunication up to Ku-band. Nighttime scintillation can be attributed to large-scale inhomogeneity in the F-region of the ionosphere predominantly between heights of 200 and 600 km. Daytime scintillation has been attributed to sporadic E. It can be thought of as occurring in three belts: equatorial, high-latitude, and mid-latitude, in order of severity. Equatorial scintillation occurs between magnetic latitudes ± 25 degrees, peaking near ± 10 degrees. It commonly starts abruptly near 2000 local time and dies out shortly after midnight. There is a strong solar cycle dependence and a seasonal preference for the equinoxes, particularly the vernal one. Equatorial scintillation occurs more frequently on magnetically quiet than on magnetically disturbed days in most longitudes. At the peak of the sunspot cycle scintillation depths as great as 20 dB have been observed at L-band.

1. Introduction.

This paper is designed to respond to the question "What additional problems does one have due to equatorial scintillation when operating satellite systems with equatorial earth stations at L-band". With this objective in mind we review the intensity, geomorphology and temporal characteristics of equatorial scintillations, discuss the indices which experimenters use to measure ionosphere scintillation, and look at currently available models. As the paper is aimed at non-ionosphericists, an effort is made to keep it as simple and applications-oriented as possible.

1.1 Background.

Ionospheric scintillation was first recognized in the mid-forties (Flock 1987). Interestingly enough, the early observations of scintillation were of signals from radio stars - direct analogs of the earth-space transmissions of interest now. During the IGY there was special attention paid to the equatorial ionosphere and a host of strange effects were discovered which had the same temporal characteristics which we now associate with equatorial scintillation. One of these was named the "Far Eastern Anomaly" (Bateman, et al. 1959) and is illustrated in the beautiful range-time record shown in Figure 1, taken by Jim Watts on a low-latitude ionospheric scatter circuit. Note the sudden commencement of the broadened trace shortly after sundown which gradually decreases after midnight. Equatorial "bubbles" (regions of plasma deficiency) were observed at Jicamarca, Peru to follow the same temporal characteristics and were observed to rise to elevations of over a thousand km (Kelley et al. 1981, Kelley 1989). These plasma depletions are believed to be aligned along the Earth's magnetic field, have dimensions of 100-200 km east-west and several thousand km north-south, and to move eastward with velocities of 50-200 m/s. These depletion regions are then the seat of irregularities with scale sizes of meters to tens of kilometers (Johnson 1988).

Persons interested in high-latitude scintillation are referred to an excellent paper by Kersley et al. (1988) on the subject.

1.2 Geographic and Temporal Characteristics.

The oft-reproduced diagram shown in Figure 2 (Basu et al. 1988) contains a wealth of information. Solar cycle dependence is illustrated by the different depths of fading indicated for the solar maximum (up to 20 dB), and solar minimum (as low as 1 dB). The geographic extent is shown to be at least 20 degrees north and south of the equator at solar maximum, with peaks on either side of the equator. The diurnal behavior is in this figure. Scintillations start shortly after 2000 local time and decay shortly after midnight.

An ambiguity in Figure 2, as in similar earlier representations (e.g. CCIR 1986), is that the identity (geographic, geomagnetic or magnetic) of the equator is left vague. The reason for this is presumably that as worldwide measurements are not available it is difficult to generalize one's data to apply worldwide.

By geomagnetic coordinates one refers to the Earth's dipole field, as represented by a magnet placed at the center of the Earth. The total intensity F of the Earth's dipole field in gauss is given by

$$F = (0.3\ R^3/r^3)[1 + 3\ \sin^2 \Theta]^{1/2} \qquad (1)$$

where R is the Earth's radius (6371 km), r is the distance from the center of the Earth, in the same units as R, and θ is geomagnetic latitude. The axis (slightly time variant) is given for January 1988 as passing through 79.1 degrees N geographic latitude and 289.1 degrees East geographic longitude (Davies 1989). Geomagnetic latitude for the Earth is given in Figure 3. The dip I in the geomagnetic coordinate system is simply related to the geomagnetic latitude L by

$$\tan L = 0.5 \tan I \qquad (2)$$

By magnetic or dip latitude L' (Smith 1957) is meant the latitude one would obtain from the analogous expression to (2) if the true ionospheric dip I' is substituted in (2),

$$L' = \tan^{-1}(0.5 \tan I') \qquad (3)$$

Magnetic latitude for the Earth is given in Figure 4. The normal procedure for obtaining magnetic latitude is to use the smoothed value of the surface dip and enter that in equation (3). As one goes up in altitude the direction of the Earth's field will gradually approach the dipole value given by expressions (1) and (2). How rapidly that value is approached is illustrated in Figure 5. For altitudes below 3000 km the true dip is seen to be better represented by magnetic latitude.

2. Observations.

The most applicable observations are the extensive ones made at C-band (primarily at 4 GHz) at Intelsat stations and those at L-band on the 1.5 GHz signal from Marisat. There is also a limited number of recordings taken in August 1980 of L1 and L2 GPS signals (Rino et al. 1981).

2.1 Amplitude Scintillation.

Shown in Figure 6 (Fang 1988) are recordings made at Stanley, the Hong Kong Intelsat station, on March 3-4, 1988 (at the peak of the solar cycle) of two satellites: the Pacific Ocean Regional (POR) at 174 degrees E and the Indian Ocean Regional at 63 degrees E. Hong Kong was the only receiver location. It could receive POR and IOR directly at 3950 MHz and it could receive the signal uplinked to POR and IOR from Sentosa, Singapore and

Si Racha, Thailand at 6 GHz and down-linked at 4 GHz. If one assumes (as does the author) that the main effect is on the down-link (at the lower frequency) then one is faced with an eastward movement of the disturbance at the time when the sub-solar point is moving westward. This result is in agreement with spaced-antenna measurements of smaller scale inhomogeneity (Johnson 1988) but the rate of travel exceeds the 200 m/s found to be maximum in that experiment.

2.2 Phase Scintillation.

Figure 7, taken from Rino et al. (1981), is an example of data recorded during twelve consecutive evenings starting August 21, 1980 at Kwajalein Atoll. (Note that this was not a seasonal peak.) Measurements of amplitude and phase were made during scintillation periods on both the L1 (1575.42 MHz) and L2 (1227.6 MHz) signal. During periods of moderate scintillation the phase deviations on L1 exceeded 50 radians while those on L2 exceeded 75 radians. In the example shown in Figure 7 the satellite (GPS 8) rose from the southeast around 2250 local time and achieved its maximum elevation of 70 to 75 degrees around 0330.

To quote from page 256 of the article "During seven of these evening data runs, the scintillation was severe enough that the GPS 5010 receiver could not maintain lock on the signal during the early portion of the pass. When the satellite was above about 30 degrees, however, the scintillation was not severe enough to cause the receiver to break lock..."

2.3 Frequency spectrum.

By frequency spectrum is meant the prevalence of frequency components in the oscillations of the received signal under scintillation conditions. An example of this is shown in Figure 8 where it can be seen that the most dominant frequency is around 10 seconds (O.1 Hz). The prevalence of higher frequencies decays roughly as f^{-3} (CCIR 1990).

3. Dependencies.

The term "correlations" might be used here, but "dependency" seems to reflect a peak at a certain time of day or season somewhat better.

3.1 Solar Cycle.

There is a clear correlation of strong scintillation with sunspot cycle as reflected in Figure 9 (CCIR 1990). However, as pointed out by Aarons (1981) this does not mean for all months or all times of day. Aarons relates the maximum scintillation regions to the Appleton anomaly, i.e. the fact that the maximum ionization in the F-region of the ionosphere is not located at the equator but in low-latitude peaks on either side of it as is illustrated in Figure 2.

3.2 Season.

The strongest scintillation at periods of high sunspot number for stations located near the two geographical maxima in Figure 2 are in equinoctial months with the vernal equinox preferred over the autumnal (Fang 1981, Basu et al. 1998).

3.3 Diurnal.

The diurnal variation of equatorial scintillation shows a strong preference for the hours of 2000 to 0100 local time as is well illustrated by Figures 1 and 2.

3.4. Magnetic.

There are two aspects to the magnetic dependence. That concerning the dependence on geographic, dipole or dip latitude has been discussed under 1.2. The suggestion is that dip

or magnetic latitude is the better choice of the three. The other aspect is whether times of magnetic quiet or disturbance are preferred. As shown by Aarons (1981) and others there is a preference for quiet days for strong scintillation.

4. Scintillation Indices.

The quantification of scintillation indices can be attributed to Briggs and Parkin (1963). Their treatment was restricted to amplitude scintillation. They reasoned that, inasmuch as what is actually observed in recordings of satellite signals is a recorder deflection proportional to the amplitude of the received wave, measures related to the mean deviation and root-mean-square deviation were logical. These measures they denoted by S_1 and S_2 defined as follows:

$$S_1 = \frac{1}{\bar{R}} \overline{|R - \bar{R}|} \qquad \text{normalized mean deviation} \qquad (4)$$

$$S_2 = \frac{1}{\bar{R}} \left\{ \overline{(R - \bar{R}^2)} \right\}^{1/2} \qquad \text{normalized RMS deviation} \qquad (5)$$

where R is the received amplitude, $\bar{R}$ is the mean value and $\overline{R - \bar{R}}$ is the mean deviation of the sample record. The values are then normalized. Hence, S_1 is the normalized mean deviation, and S_2 is a normalized standard deviation.

The authors reasoned further that, inasmuch as satellite scintillation recordings measure power, R^2, rather than amplitude, R, two parallel indices, S_3 and S_4, should be defined:

$$S_3 = \frac{1}{\bar{R^2}} \overline{|R^2 - \bar{R^2}|} \qquad (6)$$

$$S_4 = \frac{1}{\bar{R^2}} \left\{ \overline{(R^2 - \bar{R^2})^2} \right\}^{1/2} \qquad (7)$$

In their discussion Briggs and Parkin (1963) use an index S as a measure of scintillation depth defined as:

$$S^2 = \frac{\overline{R^4} - (\bar{R^2})^2}{(\bar{R^2})^2} \qquad (8)$$

For a Rayleigh distribution, applying to the limiting case where phase deviations are large, the relationships between the indices are:

$$S_1 = 0.42\, S_4 \qquad (9)$$

$$S_2 = 0.52\, S_4 \qquad (10)$$

$$S_3 = 0.73\, S_4 \qquad (11)$$

$$S \equiv S_4 \qquad (12)$$

Whitney (1969) proposed a scintillation index, S.I., defined as:

$$S.I. = \frac{P_{max} - P_{min}}{P_{max} + P_{min}} \quad (13)$$

where P_{max} is the power amplitude of the third peak down from the maximum measured, and P_{min} is the third peak up from the minimum excursion in a 15 minute period of recording. Later usage (Yeh et al. 1981) takes the highest peak and minimum excursion instead of the third up and third down.

5. Models.

Computer modeling of equatorial scintillation was initially based on two data sets (Secan et al. 1993). The first was data collected from the Wideband satellite in the 1970s at Ancon, Peru, and Kwajalein Atoll (VHF, UHF, and L-band). The second was data collected from the Marisat satellite from Ascension Island (L-band) and Huancayo, Peru (VHF), and from the Fleetsat satellite from Manila (VHF). The Wideband satellite data included both intensity and phase (WBMOD) and has been gradually enhanced over the years (Secan et al. 1987) to its latest version (Secan et al. 1993): "The WBMOD uses a collection of empirically derived models to describe the global distribution and behavior of naturally occurring ionospheric irregularities, and a power-law phase-screen propagation model to calculate estimates of the level of intensity and phase scintillation that these irregularities would impose on a user-defined system and geometry." Details of this code can be obtained from James A. Secan, Northwest Research Associates, Inc. P.O. Box 3027, Belleview, Washington 98009.

6. References

Aarons, J. (1981) Microwave equatorial scintillation intensity during solar maximum. 193-201, **Proceedings of the Ionosphere Effects Symposium 1981**, U.S. Gov't Printing Office.

Basu, Sa., E. MacKenzie, and Basu, Su. (1988). Ionospheric constraints on VHF/UHF communications links during solar maximum and minimum periods, **Radio Sci.**, **23**, 363-378, May-June.

Bateman, R., J.W. Finney, E.K. Smith, L.H. Tveten, and J.M. Watts (1959). IGY observations of F-layer scatter in the Far East, **J. Geophys. Res.**, **64**, 403-405.

Briggs, B.H., and I.A. Parkin (1963). On the variation of radio star and satellite scintillation with zenith angle. **J. Atmos. Terr. Phys. 26**, 1-23.

CCIR (1986). Ionosphere effects upon earth-space propagation, Report 263-6, **vol. 6: Propagation in Ionized Media of CCIR XXVIth Plenary Assembly**, ITU Geneva.

CCIR (1990) Ionosphere effects upon earth-space propagation, Report 263-7, **Annex to vol. 6: Propagation in Ionized Media of CCIR XXVIIth Plenary Assembly**, ITU Geneva.

Davies, K. (1989). **Ionospheric Radio**, Peter Peregrinus, Ltd. on behalf of the IEE.

Fang, D.J. (1981). C-band ionospheric scintillation measurements at Hong Kong Earth station during the peak of solar activity in sunspot cycle 21, 181-192, **Proceedings of the Ionosphere Effects Symposium 1981**, U.S. Gov't Printing Office.

Fang, D.J. and M.S. Pontes (1981). 4/6 Ghz ionospheric scintillation measurements during the peak of sunspot cycle 21, **COMSAT Tech. Rev. 11**, No. 2, 293-320.

Flock, W.L. (1987). **Propagation Effects on Satellite Systems at Frequencies Below 10 GHz - A Handbook for Satellite System Design**. NASA Reference Publication 1108(02).

Kelley, M.C. (1989). **The Earth's Ionosphere - Plasma Physics and Electrodynamics**. Academic Press

Kelley, M.C., M.F. Larson, C.A. LaHoz, and J.P. McClure (1981). Gravity wave initiation of equatorial spread F. **J. Geophys. Res. 86**, 9087.

Kersley, L., S.E. Pryse, and N.S. Wheadon (1988). Amplitude and phase scintillation at high latitudes over Europe, **Radio Sci. 23**, 320-330 (May-June)

Johnson, A.L. (1988). Short-term magnetic field alignment variations of equatorial ionospheric irregularities, **Radio Sci. 23**, 331-336, May-June.

Johnson, F.S. (1961). **Satellite Environment Handbook**, Stanford University Press.

Mollen, T.A., C.H. Liu and D.J. Fang (1988). A study of C-band equatorial scintillation in the Asian sector, **Radio Sci. 23**, 337-345, May-June.

Rino, C.L., M.D. Cousins, and J.A. Klobuchar (1981). Amplitude and phase scintillation measurements using the Global Positioning System, 253-261 of **Proceedings of the Ionosphere Effects Symposium 1981**, U.S. Gov't Printing Office.

Secan, J.A., E.J. Fremouw, and R.E. Robins (1987). A review of recent improvements to the WBMOD ionospheric scintillation model. 607-616, **Effect of the Ionosphere on Communications, Navigation, and Surveillance Systems**, J. Goodman, Ed., U.S. Gov't Printing Office.

Secan, J.A., R.M. Bussey, E.J. Fremouw, and Sa. Basu (1993). An improved model of equatorial scintillation, **Proceedings of the Ionosphere Effects Symposium 1993**, U.S. Gov't Printing Office.

Smith, E.K. (1957). Magnetic latitude derived from the dip angle, Appendix III of **Worldwide Occurrence of Sporadic E**, NBS Circular 582, U.S. Gov't Printing Office.

Smith, E.K. (1974). ***A Study of Ionospheric Scintillation As It Affects Satellite Communication***. OT Technical Memorandum 74-186, U.S. Department of Commerce.

Whitney, H.E. (1969). The definition of scintillation index and its use for characterizing ionospheric effects, 3-5, **AGARD Report 571**, Jules Aarons, Ed.

Yeh, K.C., J.P. Mullen, J.R. Medeiros, R.F. da Silva and R.T. Medeiros (1981). Ionospheric scintillation observations at Natal, 202-209, **Proceedings of the Ionosphere Effects Symposium 1981**, U.S. Gov't Printing Office.

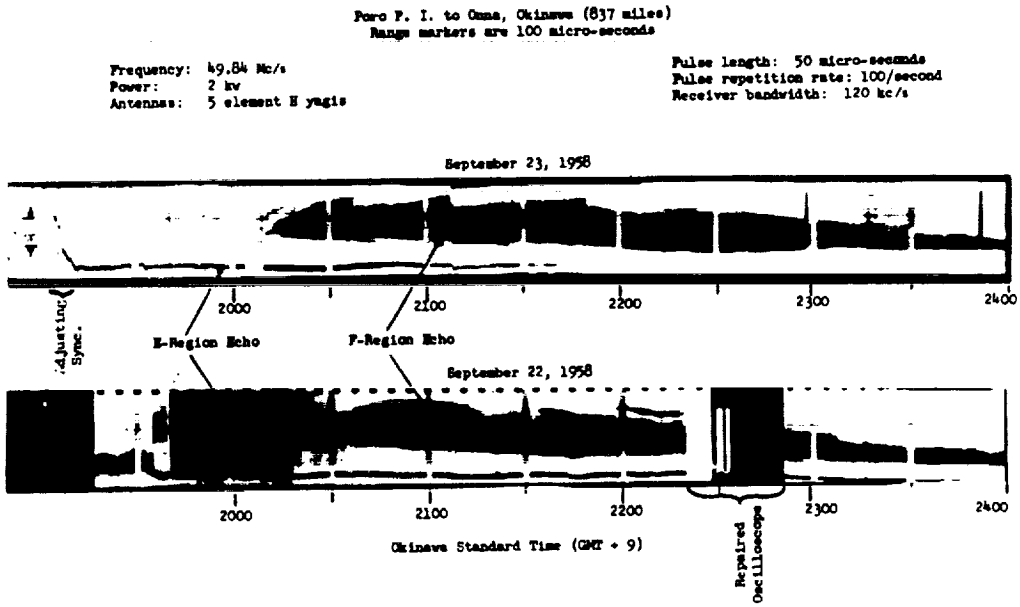

Figure 1. The "Far Eastern" or evening signal anomaly; after Bateman et. al., 1959)

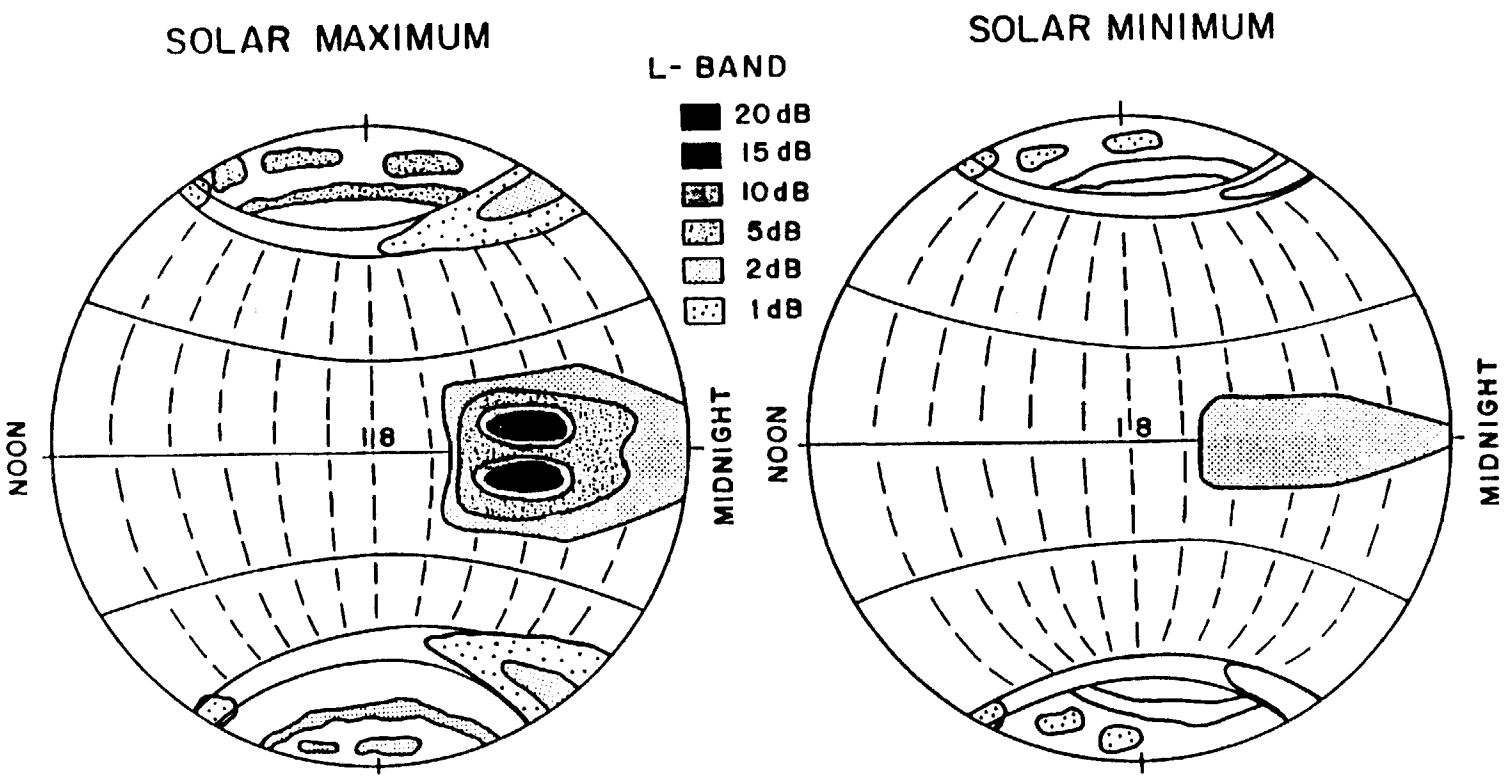

Figure 2. Illustrative picture of scintillation occurrence based on observations at L-band (1.6 GHz); after Basu et al. 1988.

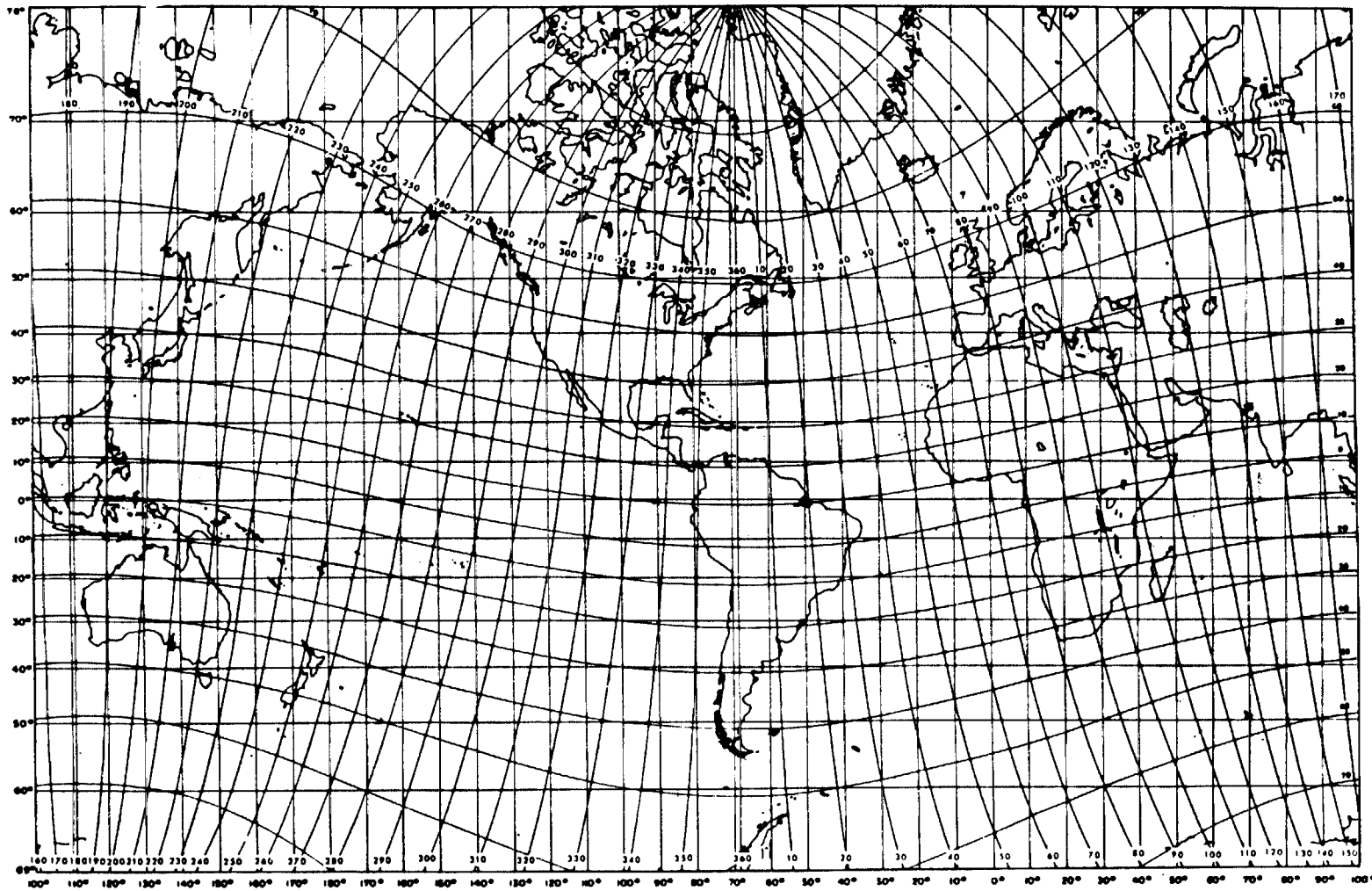

Figure 3. Geomagnetic dipole field coordinate grid superimposed on a Mercator projection of the world; after Johnson 1961.

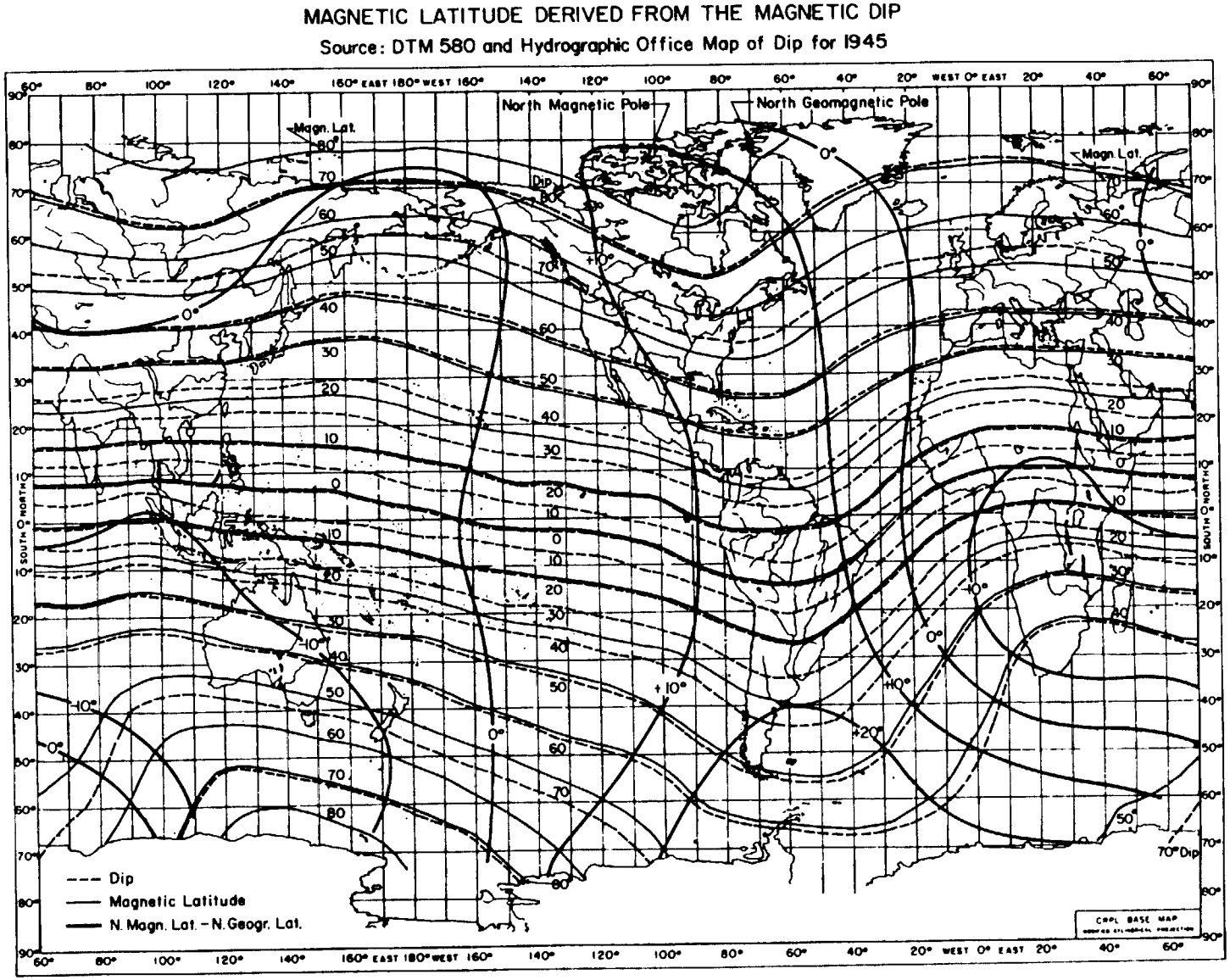

Figure 4. Magnetic latitude derived from the observed dip, epoch 1955; after Smith 1957.

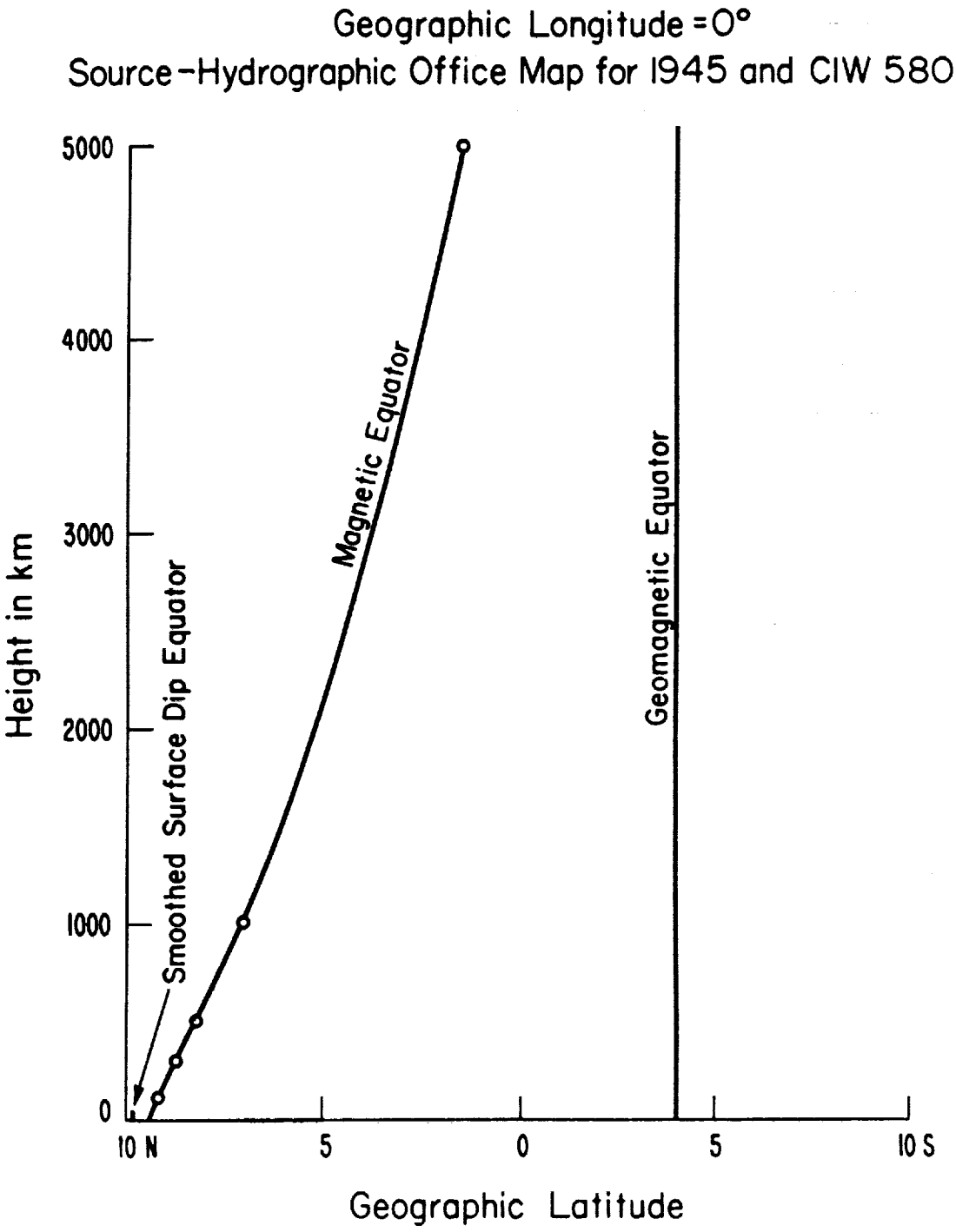

Figure 5. Comparison of the surface magnetic equator with the geomagnetic equator as a function of altitude above the earth; after Smith 1957.

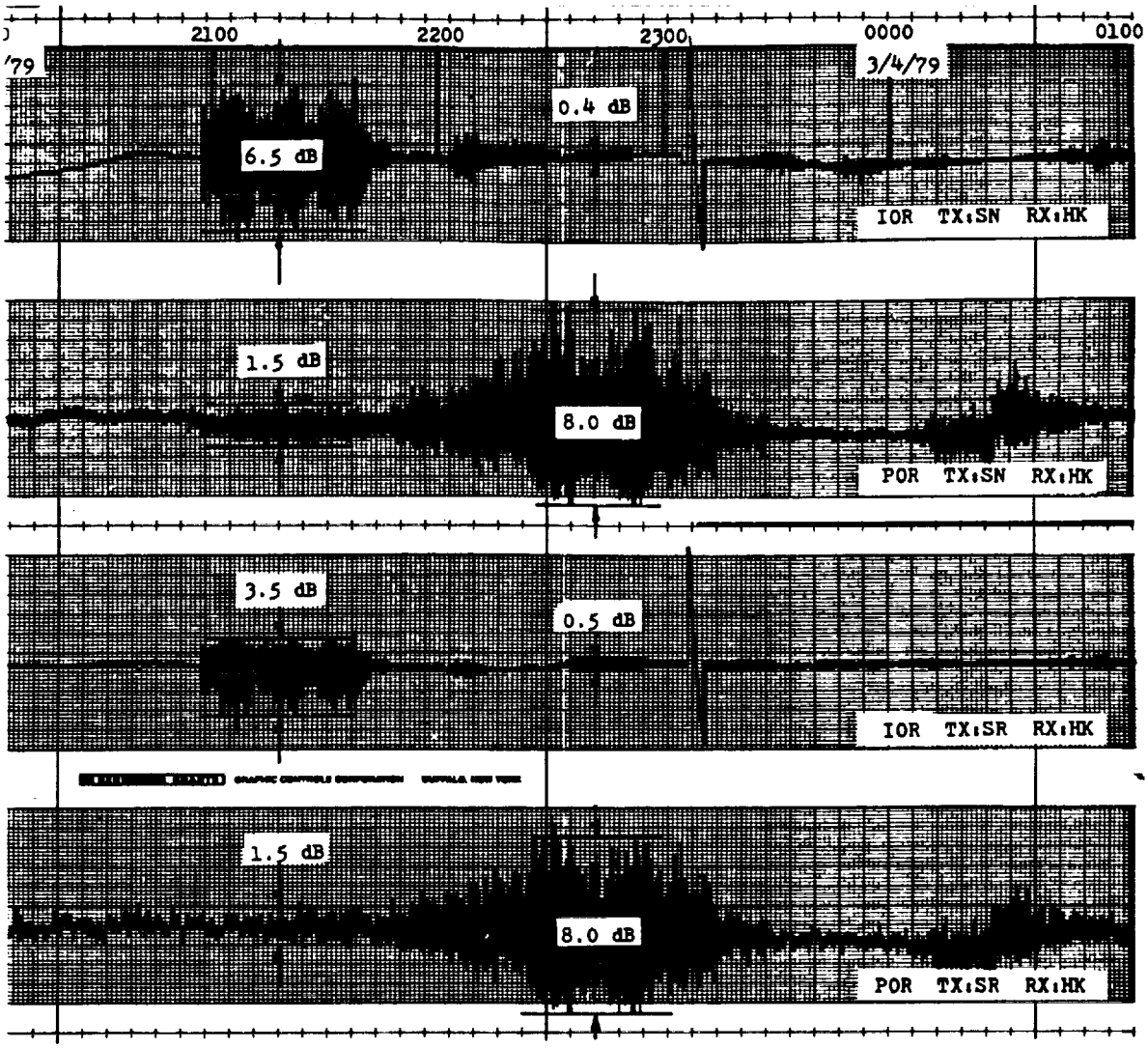

Figure 6. Records of C-band ionospheric scintillation on March 3-4, 1979 from Hong Kong; after Fang 1981.

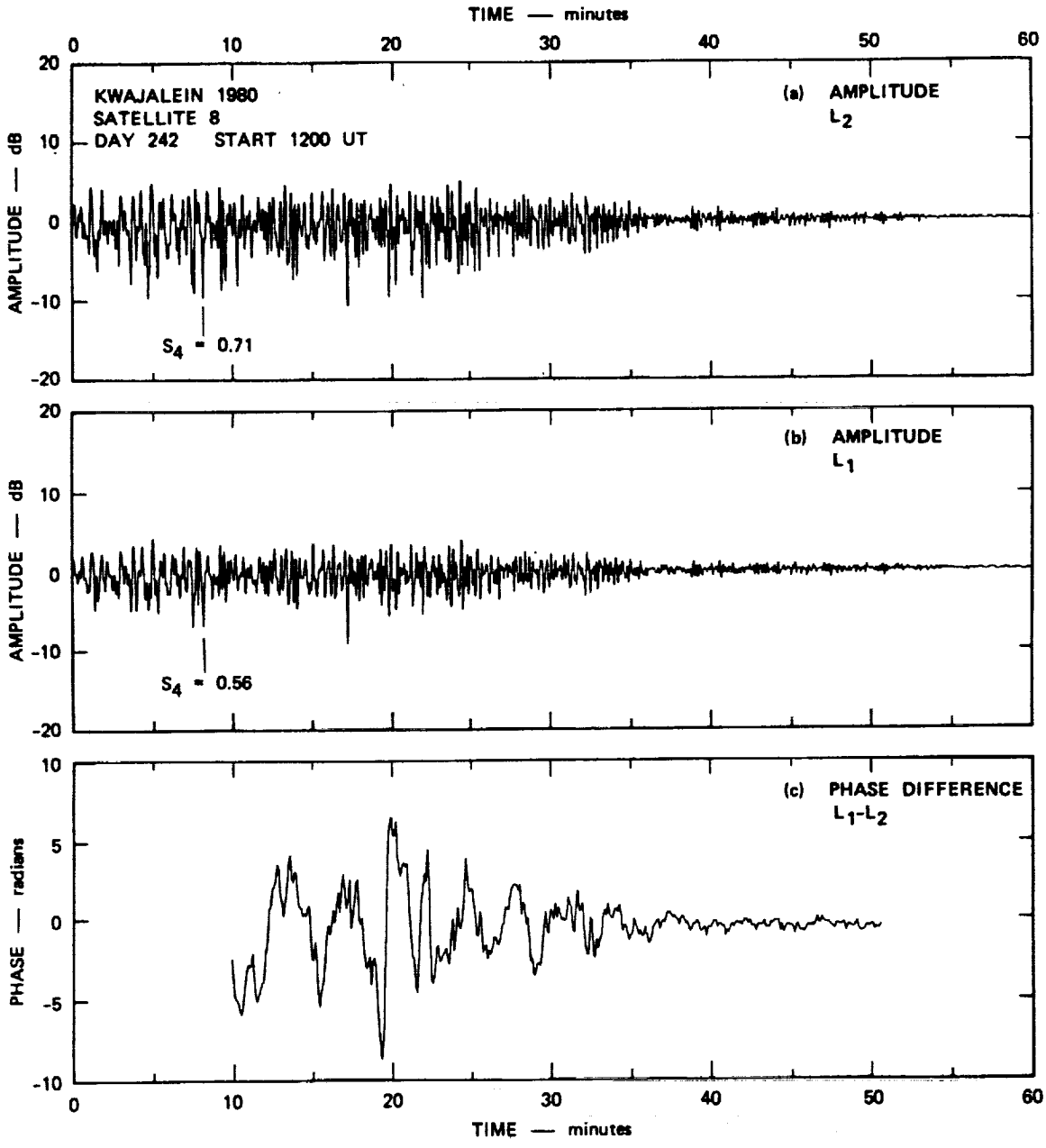

Figure 7. Example of strong L-band scintillation and decay on GPS signals; after Rino et al. 1981.

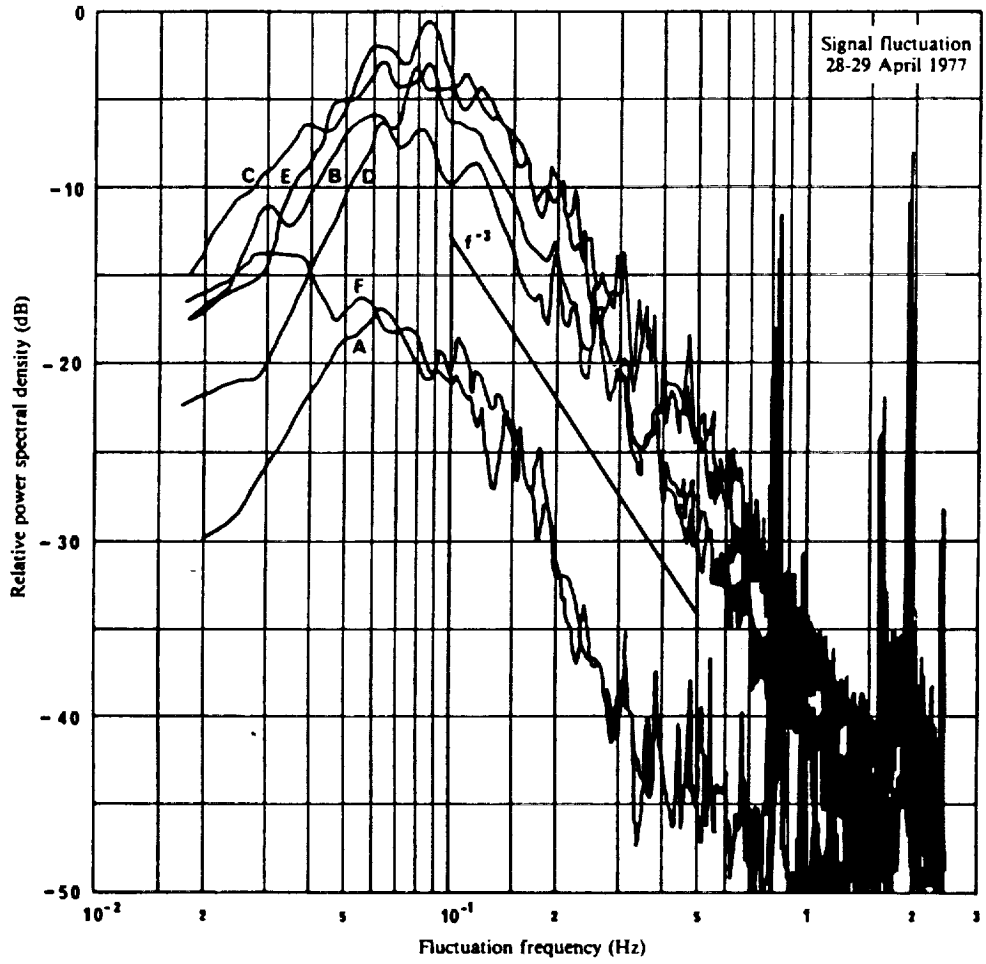

Figure 8. Power spectral density estimates for a geostationary satellite (Intelsat 4) at 4 GHz.; after CCIR 1990.

The scintillation event was observed during the evenings of 28-29 April 1977 at Taipei Earth Station

A: 30 minutes before event onset
B: at the beginning
C: 1 hour after
D: 2 hours after
E: 3 hours after
F: 4 hours after

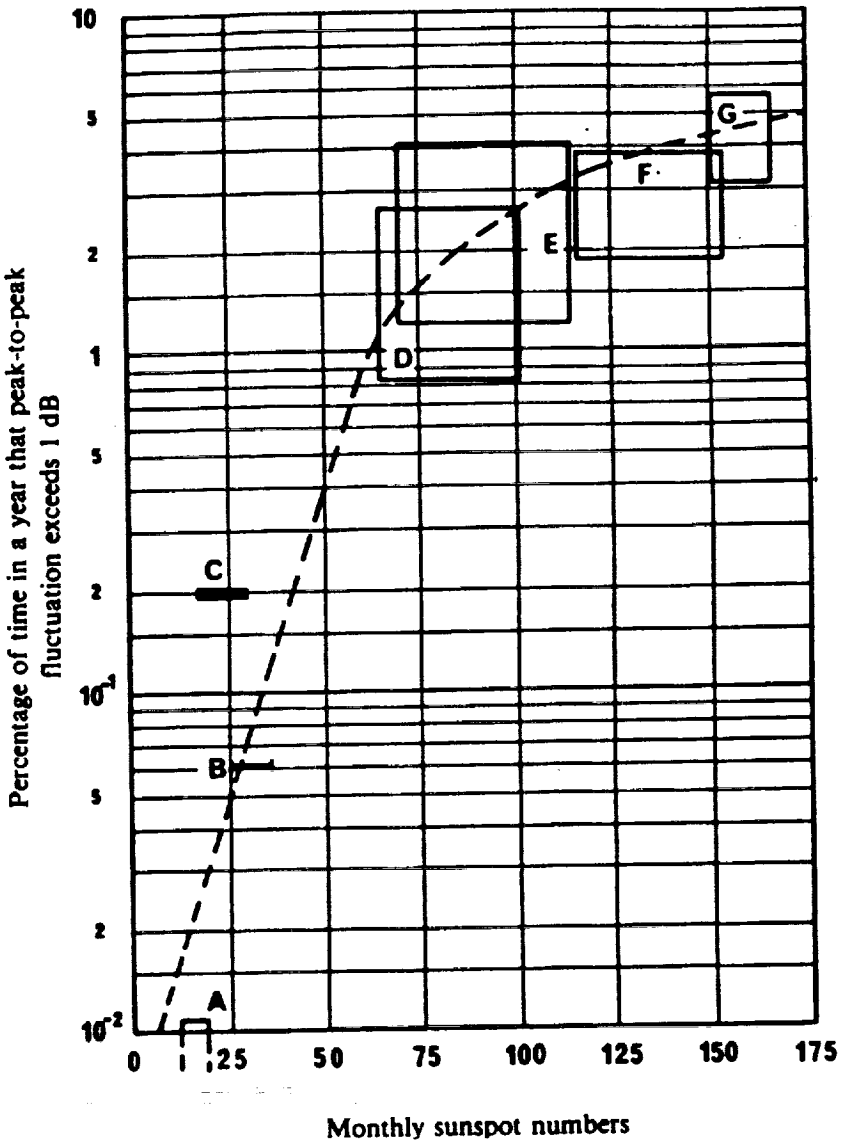

Figure 9. Dependence of 4 GHz equatorial scintillation on sunspot number; after Fang 1980, Fang and Pontes 1981

The bars and squares are the ranges of variations over a year for different carriers.

A: 1975-1976, Hong-Kong and Bahrein, 15 carriers
B: 1974, Longovilo, 1 carrier
C: 1976-1977, Taipei, 2 carriers
D: 1970-1971, 12 stations, > 50 carriers
E: 1977-1978, Hong-Kong, 12 carriers
F: 1978-1979, Hong-Kong, 10 carriers
G: 1979-1980, Hong-Kong, 6 carriers